New Strategy for Stark Deceleration

David Reens,* Hao Wu, Alexander Aeppli, Anna McAuliffe, Piotr Wcisło, Tim Langen,† and Jun Ye
JILA, National Institute of Standards and Technology and the University of Colorado and Department of Physics, University of Colorado, Boulder, Colorado 80309-0440, USA
(Dated: June 26, 2019)

Since its first realization, Stark deceleration has unlocked incredible new opportunities for the control of molecular beams. Numerous trapping and collisional studies have been performed, and several important extensions to the technique have been developed. Nevertheless, Stark deceleration has thus far been prevented from realizing its full potential due to significant limitations in the performance of the deceleration strategies thus far utilized. We introduce a new strategy that offers many-fold performance improvements across all useful operating conditions for a Stark decelerator, including an order of magnitude increase in molecule number at trappable final velocities. Our strategy also makes the application of Stark deceleration to less readily polarized species and to longer devices much more feasible.

Over the past two decades, Stark deceleration has enabled groundbreaking collisional [1–3] and spectroscopic [4–7] studies of a variety of species [8]. Subsequent trap-loading greatly enhances interrogation time for such studies [9] and opens the door for further cooling and manipulation [10, 11]. Alongside the history of achievements enabled by Stark deceleration runs a parallel ongoing saga surrounding their efficient operation. Many important steps have been made, not only in understanding the flaws of the canonical pulsed decelerator [12, 13], but also in addressing them through the use of overtones [14, 15], undertones [16], or even mixed phase angles [17, 18]. Even with these advances, the outstanding inefficiencies of the pulsed decelerator, particularly with regard to transverse phase stability, have motivated alternative geometries such as interspersed quadrupole focusing [13] and traveling wave deceleration [19–21]. Although traveling wave deceleration takes a strong step toward truly efficient operation, it comes with costs in system complexity. These costs can be partially addressed by the use of combination pulsed and traveling wave devices [22], or even using traveling wave geometry with pulsed electronics [23, 24]. In Zeeman deceleration, a parallel saga exists, with early demonstrations [25, 26] later improved through the use of anti-Helmholtz configurations with better transverse focusing properties [27, 28]. Lacking a comparable breakthrough for Stark devices, others continue to pursue brand new geometries [29], or even combine the best features of Stark and Zeeman approaches in a single device [30, 31]. Our strategy works with conventional geometry and electronics, but fully resolves transverse challenges and offers more than tenfold gains even at very low speeds.

The strategy is to mix new field distributions into the deceleration process that feature strong restoring force in the transverse directions. Depending on which field distributions are admixed, we specify several operating modes employing this strategy: focusing (F), strong focusing (SF), and very strong focusing (VSF). The measured performance of these modes against the $S=1$ and

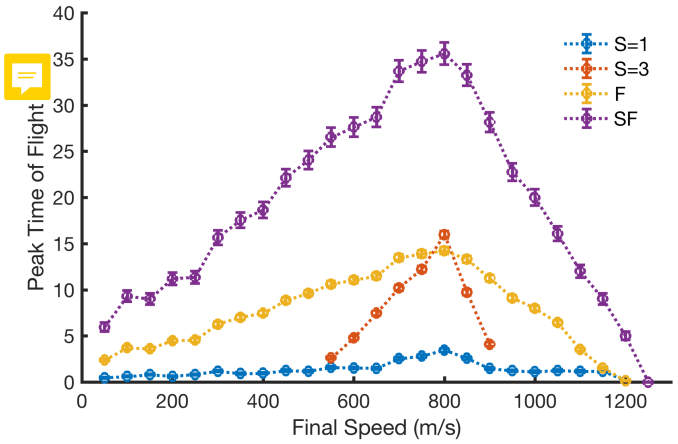

FIG. 1. Experimental comparison of deceleration strategies. Data are collected with a 333 stage decelerator and a beam of OH radicals expanded in Neon at an initial speed of 820 m/s. Large gains persist at low speeds, with SF, an operating mode employing the new strategy, outperforming $S=1$ at 50 m/s elevenfold. Larger accelerations than decelerations are possible in the device, demonstrating the increased range of SF mode.

$S=3$ operating modes which employ the conventional strategy is shown in Fig. 1 for hydroxyl radicals, a benchmark species for Stark deceleration. These are performed on a decelerator not previously reported, with 2 mm pin spacing and other geometric parameters as in our earlier devices [32, 33], but with more than double the length, 333 stages, so as to be suitable for decelerating a beam seeded in room temperature neon to rest. F mode, which requires no wiring changes and may be immediately employed on existing devices already enhances performance by a factor of $4-8$. With some investment in high voltage equipment, we also implement SF mode, providing an additional significant gain. A comparable investment would enable VSF mode, but we do not pursue this since it is less useful for trapping, our primary emphasis, for reasons discussed further below. The slowest speeds shown are typical in a system such as ours designed to provide molecules that are one pulse away from being trapped.

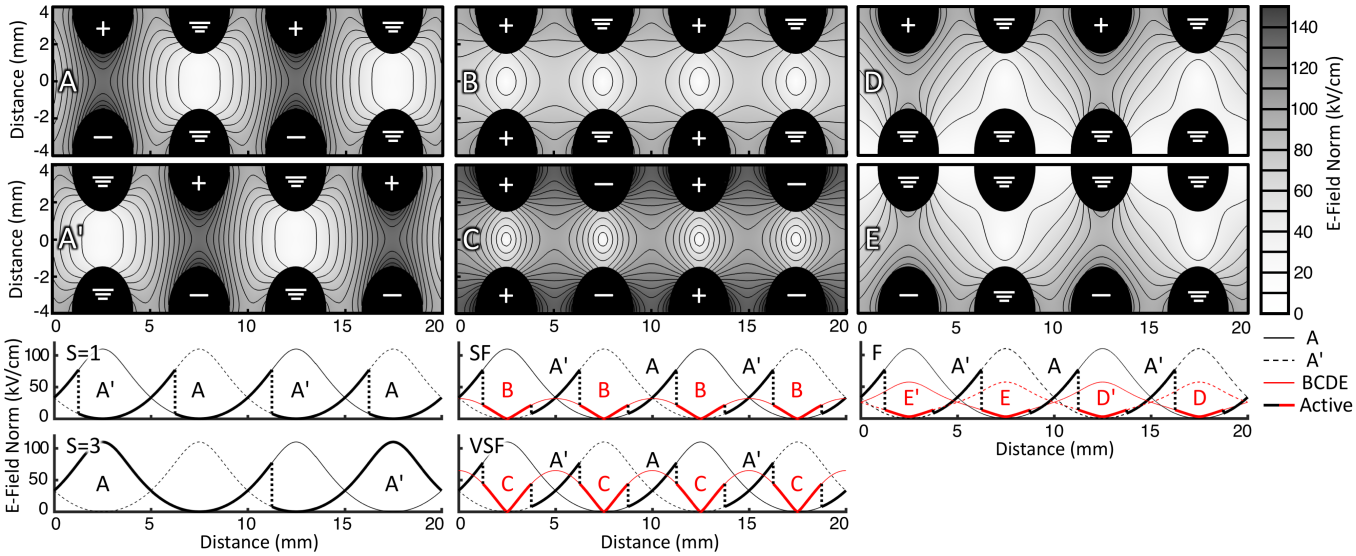

FIG. 2. A new strategy for Stark deceleration, consisting of novel distributions of the electric field and operation modes which employ them. Distributions B-E feature strong transverse focusing where molecules would normally pass between grounded pin pairs. On-axis energy diagrams are shown for operation modes named focusing (F), strong focusing (SF), and very strong focusing (VSF). These incorporate Distributions D/E, B, and C respectively. Primes indicate translation to the next pin pair. Conventional operating modes S = 1,3 [14], are also shown.

The reason for the dramatic success of this new deceleration strategy may be understood as follows. In the conventional strategy [8], molecules approach a charged pin pair, climbing a hill in potential energy. The hill is abruptly switched off, allowing molecules to then repeat the process without regaining that potential energy. The abrupt switch occurs partway up the potential energy hill, so that molecules that are ahead get more energy removed, and vice versa. This creates a traveling potential well for the molecules, with a longitudinal restoring force towards the center of a decelerating reference frame whose deceleration is set by the chirp rate of the switching frequency. It is customary to define an idealized "synchronous molecule" with zero energy with respect to this potential well, which proceeds exactly down the central axis of the decelerator and climbs each potential hill to the same position at the moment of a switching event. In the transverse directions, restoring force is not inherited from switching events, but arises directly from the focusing properties of field distributions in the lab frame. Pins are always charged in bipolar pairs, in which case transverse focusing occurs right between the charged pin pair, but not significantly elsewhere (Fig. 2, A). This causes molecules to experience much better transverse focusing when they are regularly sampling the focusing fields right between the charged pin-pair, which requires them to be oscillating regularly ahead and behind the synchronous molecule.

Just after the switching event, which as mentioned must happen only partway up the potential energy hill, molecules proceed through the largely field-free region between grounded pin pairs. This region is of central importance to our new deceleration strategy. Useful field distributions with transverse focusing in this region can be created by applying voltage in a way that is not balanced between adjacent pin pairs (Fig. 2, B–E). This imbalance causes field lines to run toward the grounded pin pair, creating a focusing 2D quadrupole structure, much like this one used intentionally for trapping and controlling spin-flip losses [11]. By implementing these distributions when the synchronous molecule is flying between the grounded pin pair, but retaining the use of the conventional distribution otherwise, the longitudinal behavior of the device is preserved while the transverse behavior is vastly improved. We identify several operational modes employing this strategy, varying according to the magnitude of their transverse focusing effects. Utilizing the field distribution arising from charging only a single rod, something readily achievable with no change to high voltage electronics, gives rise to a focusing mode (F). Charging two pins to the same voltage gives rise to strong focusing (SF), and charging all four pins, one pair at one voltage and the next pair at the opposite voltage, gives very strongly focusing (VSF).

In order to quantitatively analyze these operation modes, we can work in the decelerating non-inertial frame of the molecules, where a traveling potential well is generated with deceleration included as a fictitious force. Traveling wells generated by various operation modes may be visually inspected by plotting equipotential surfaces at various potential energies relative to the well minimum, see Fig. 3b. These are calculated as described ~~here~~ [36], where the same treatment as in [34, 35] is performed but with extension to three dimensions. At some minimum

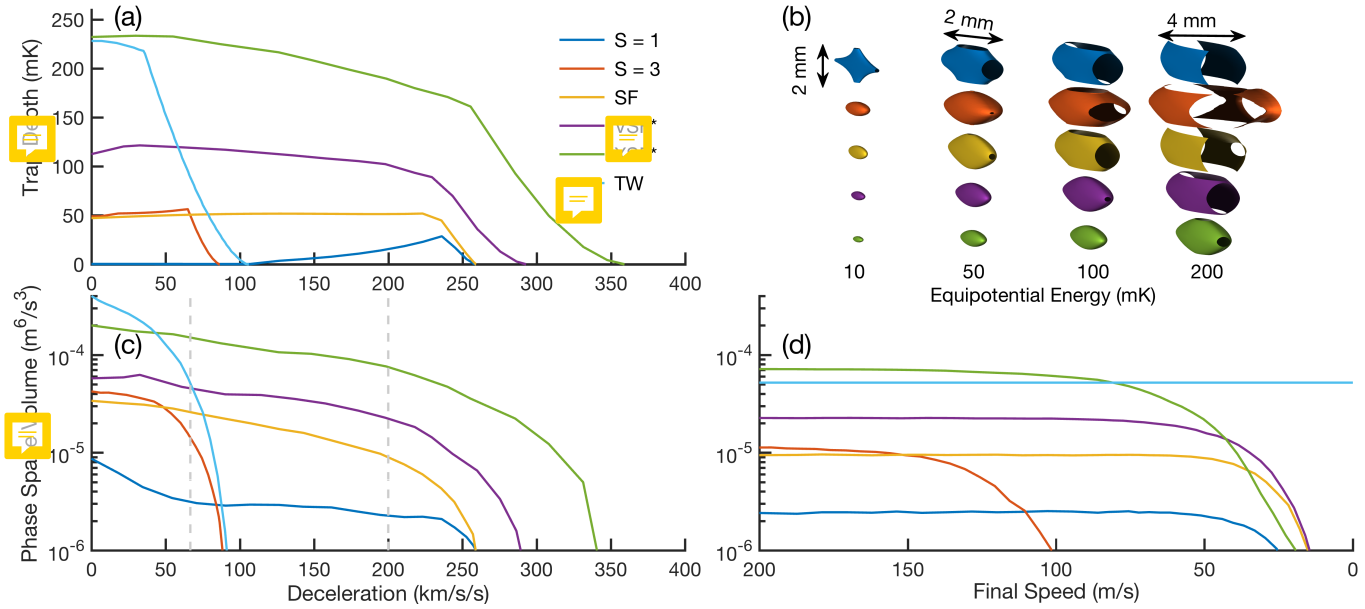

FIG. 3. The traveling potential well under different modes of operation. Conventional S = 1 and S = 3 modes, together with modes F, SF, and VSF employing the new strategy. Traveling wave (TW) deceleration is also compared, assuming a 10 kV peak to peak waveform. (a) Minimum escape energy as a function of deceleration. (b) Equipotentials of the traveling well for 150 km/s/s deceleration, 50 km/s/s for S = 3. Lack of closure of an equipotential equates to possibility of escape. (c) Initial phase space volume remaining within the traveling well after 3 ms, only the effective traveling well is simulated. (d) Full decelerator simulation, agreeing with (c) at high enough final speeds, studied with varying final velocity but with hold time fixed at 3 ms and deceleration fixed as indicated by the gray dashed lines in panel (c). For TW a full simulation is not performed; the value corresponding to 67 km/s/s in panel (c) is shown for comparison.

escape energy $E_{\rm esc}$, the traveling well equipotential fails to be closed, enabling molecules with energy $E \geq E_{\rm esc}$ to escape. This escape may occur transversely, after which molecules encounter the surfaces of decelerator pins and are lost, or longitudinally, where molecules are not immediately lost but cease to remain in close proximity to the synchronous molecule. $E_{\rm esc}$ is plotted for all modes and as a function of varying decelerations in Fig. 3a. $E_{\rm esc}$ is a useful figure of merit for characterizing the performance of a given operating mode, as evidenced by the close agreement between Fig. 3a and Fig. 3c, where the molecule number remaining in the traveling well after a 3 ms hold time is reported.

For the S = 1 mode, $E_{\rm esc}$ is nearly zero, particularly for molecules which move away from the trap center along the x and y axes. This is the underlying reason for the transverse-longitudinal coupling problem that has been described [12]. In general, such couplings are often useful for maintaining ergodicity in a potential well [37], but with some directions featuring very low escape energy, even small amounts of motional coupling lead to loss. $E_{\rm esc}$ actually improves with stronger deceleration for S = 1, as expected given the increased sampling of the transversely focusing region when molecules climb further towards the charged pin pair, see Fig. 2A. Remarkably, F mode offers comparable $E_{\rm esc}$ to S = 3, but with no sacrifice in deceleration capability. The SF and VSF modes make more dramatic improvements, with the latter rivaling traveling wave (TW) deceleration [19]. In Fig. 3, 10 kV peak to peak sine waves are assumed, to our knowledge the largest used to decelerate all the way to rest. Additionally, all modes besides TW use the rather small 2x2 mm^2 open area of our device, while TW devices use rings of 4 mm inner diameter. If VSF mode were used with a 3x3 mm^2 device [15] or a 4x4 mm^2 [38], phase space volume would increase significantly, depending approximately on the cube of pin-pair spacing.

The domain of validity of the use of traveling wells to characterize deceleration is a key concern. More commonly the traveling well approach is reserved for continuous deceleration schemes [19, 26]. Essentially, it is required that the longitudinal velocity v_z of the molecules satisfy $v_z/D >> f$, D the stage distance and f the oscillation frequency in the traveling well. The precise dynamics as one approaches this bound are relevant, especially for trapping experiments, which necessarily violate this condition as $v_z \to 0$. These dynamics may be precisely isolated by comparing the simulation of molecules in the traveling well (Fig. 3c) to full Monte-Carlo simulations of the deceleration. By varying only the final speed, and keeping deceleration and run-time exactly fixed by appropriately varying initial speed and decelerator length, we obtain the results shown in Fig. 3d. The asymptotically flat profiles at high enough speeds validate the traveling well approach, as do the quantitative agreement between the asymptotic values and the corre-

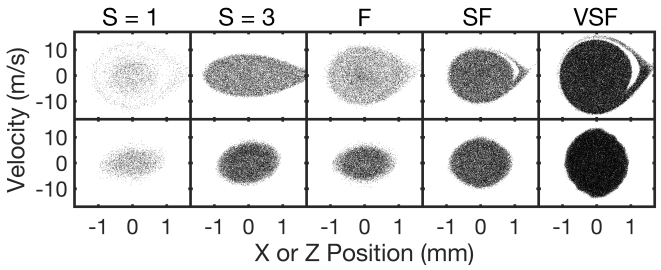

FIG. 4. Phase Space Fillings, both longitudinal (above) and transverse (below), for the labeled operation modes. With the same uniformly distributed initial phase space, the surviving number of molecules is 3, 17, 11, 24, and 75 thousand respectively. Note dramatic improvements in homogeneity and flux, without significant broadening to larger velocity classes except for VSF. Molecules travel 333 stages, begin at 900 m/s, and slow at 200 km/s/s (67 km/s/s for S = 3) to a final speed above 200 m/s.

sponding points at 200 km/s/s and 67 km/s/s in Fig. 3c.

The beginning of the low-speed breakdown depends on the intended use of the decelerator, and especially how far the molecules will be expected to travel unguided afterwards. In Fig. 3c, the molecules still confined within a 3 mm diameter circle transversely after 5 mm free flight from the end of the sequence are shown. This is a conservative representation of what is required for trap-loading, but for collisional experiments a larger flight distance may be required. Note how F and SF cut off at even lower speeds than S = 1, but VSF cuts higher. This can be attributed to the fact that VSF actually features an increased transverse trap frequency relative to the others, while F and SF improve over S = 1 mostly by mitigation of escape minima, and not by increasing the transverse confinement strength of the well. VSF mode may be especially useful for trap loading in combination with a TW device as in [22].

In Fig. 4, the longitudinal and transverse phase space fillings are compared for all modes, with 200 km/s/s deceleration through our 333 stage device, and final speeds of about 200 m/s to neglect cutoff behavior. As can be seen, the distribution is nearly homogeneous for all modes except S = 1. Increases in apparent density between panels do not arise from actual phase space density increases, but from increases in phase space volume which manifest as density after the ensemble is projected onto a plane.

All modes are initialized with the same homogeneous phase space density, which is valid for an initial beam source with a characteristic temperature larger than that of the traveling potential well. In the longitudinal direction, most supersonic expansions satisfy this, with the exception of those performed with Helium buffer gas, which can reach temperatures as low as 40 mK expanding from room temperature [39]. For this work, OH expands in neon and reaches a 300 mK longitudinal temperature [40]. In the transverse direction, source temperature is a more subtle phenomenon, and may be bimodal [41]. Furthermore, beam skimming and the resulting interference it causes often require increased distance between the source and the decelerator, resulting in poor phase space matching and a transversely under-filled effective trap. It follows that fully leveraging the transverse phase space attainable with VSF mode will likely require skimmer cooling [40].

It is observed that SF and VSF mode feature a very close match between their longitudinal and transverse phase space acceptances. This is a consequence of the tuning of an extra parameter afforded by the new deceleration modes- the relative time devoted to the original field distributions (Fig. 2, A, A') and those with increased transverse focusing (Fig. 2, B–E). In all mode diagrams shown in Fig. 2, new field distributions are applied over a spatial region that is exactly centered around the grounded pin pair. But if this restriction is lifted, a new tuning parameter arises, a second phase angle ϕ_2 of sorts. In Fig. 3, ϕ_2 is tuned for SF and VSF so as to maximize the escape energy for each deceleration. These tuned versions are labeled as SF* and VSF*, and the optimum ϕ_2 are listed in [36]. This escape energy is usually maximized when the transverse and longitudinal depths are made comparable, since otherwise one direction is limiting, hence the similar shape of the transverse and longitudinal distributions. Tuning ϕ_2 for maximum escape energy tends to optimize flux as well, but one could instead tune for a desired ratio of longitudinal to transverse spread as required for optimal collisional studies or phase space matching to a trap.

A new deceleration strategy has been introduced, with several accompanying modes of operation for the conventional pulsed decelerator. Significant improvements in transverse focusing and overall performance are obtained. This strategy does not simply increase the temperature of molecules which may be decelerated. Instead, by increasing the minimum escape energy E_{esc} from the traveling potential well, a greater flux of molecules at the same temperatures as before is obtained. This discovery opens up brand new possibilities for applying Stark deceleration to much faster beams or to molecules with less favorable Stark shift to mass ratios, since decelerator lengths and runtimes may now be extended without suffering from transverse trap leakage.

* dave.reens@colorado.edu.
† Present Address: 5. Physikalisches Institut and Center for Integrated Quantum Science and Technology (IQST), Universität Stuttgart, Pfaffenwaldring 57, 70569 Stuttgart, Germany

[1] B. C. Sawyer, B. K. Stuhl, M. Yeo, T. V. Tscherbul, M. T. Hummon, Y. Xia, J. Kłos, D. Patterson, J. M. Doyle, and J. Ye, Physical Chemistry Chemical Physics

13, 19059 (2011).
[2] M. Kirste, X. Wang, H. C. Schewe, G. Meijer, K. Liu, A. van der Avoird, L. M. C. Janssen, K. B. Gubbels, G. C. Groenenboom, and S. Y. T. van de Meerakker, Science **338**, 1060 (2012).
[3] Z. Gao, T. Karman, S. N. Vogels, M. Besemer, A. van der Avoird, G. C. Groenenboom, and S. Y. T. van de Meerakker, Nature Chemistry **10**, 469 (2018).
[4] J. Veldhoven, J. K upper, H. L. Bethlem, B. Sartakov, A. J. A. Roij, and G. Meijer, The European Physical Journal D **31**, 337 (2004).
[5] E. R. Hudson, H. J. Lewandowski, B. C. Sawyer, and J. Ye, Physical Review Letters **96**, 143004 (2006).
[6] B. L. Lev, E. R. Meyer, E. R. Hudson, B. C. Sawyer, J. L. Bohn, and J. Ye, Physical Review A **74**, 061402 (2006).
[7] A. Fast, J. E. Furneaux, and S. A. Meek, Physical Review A **98**, 052511 (2018).
[8] S. Y. T. van de Meerakker, H. L. Bethlem, N. Vanhaecke, and G. Meijer, Chemical Reviews **112**, 4828 (2012).
[9] B. C. Sawyer, B. K. Stuhl, D. Wang, M. Yeo, and J. Ye, Physical Review Letters **101**, 203203 (2008).
[10] B. K. Stuhl, M. T. Hummon, M. Yeo, G. Quéméner, J. L. Bohn, and J. Ye, Nature **492**, 396 (2012).
[11] D. Reens, H. Wu, T. Langen, and J. Ye, Physical Review A **96**, 063420 (2017).
[12] S. Y. T. van de Meerakker, N. Vanhaecke, and G. Meijer, Annual Review of Physical Chemistry **57**, 159 (2006).
[13] B. C. Sawyer, B. K. Stuhl, B. L. Lev, J. Ye, and E. R. Hudson, European Physical Journal D **48**, 197 (2008).
[14] S. Y. T. van de Meerakker, N. Vanhaecke, H. L. Bethlem, and G. Meijer, Physical Review A **71**, 053409 (2005).
[15] L. Scharfenberg, H. Haak, G. Meijer, and S. Y. T. van de Meerakker, Physical Review A **79**, 023410 (2009).
[16] D. Zhang, G. Meijer, and N. Vanhaecke, Physical Review A **93**, 023408 (2016).
[17] L. P. Parazzoli, N. Fitch, D. S. Lobser, and H. J. Lewandowski, New Journal of Physics **11**, 055031 (2009).
[18] S. Hou, S. Li, L. Deng, and J. Yin, Journal of Physics B: Atomic, Molecular and Optical Physics **46**, 045301 (2013).
[19] A. Osterwalder, S. A. Meek, G. Hammer, H. Haak, and G. Meijer, Physical Review A **81**, 051401 (2010).
[20] J. van den Berg, S. Mathavan, C. Meinema, J. Nauta, T. Nijbroek, K. Jungmann, H. Bethlem, and S. Hoekstra, Journal of Molecular Spectroscopy **300**, 22 (2014).
[21] M. I. Fabrikant, T. Li, N. J. Fitch, N. Farrow, J. D. Weinstein, and H. J. Lewandowski, Physical Review A **90**, 033418 (2014).
[22] M. Quintero-Pérez, P. Jansen, T. E. Wall, J. E. van den Berg, S. Hoekstra, and H. L. Bethlem, Physical Review Letters **110**, 133003 (2013).
[23] S. Hou, Q. Wang, L. Deng, and J. Yin, Journal of Physics B: Atomic, Molecular and Optical Physics **49**, 065301 (2016).
[24] Y. Shyur, J. A. Bossert, and H. J. Lewandowski, Journal of Physics B: Atomic, Molecular and Optical Physics **51**, 165101 (2018).
[25] N. Vanhaecke, U. Meier, M. Andrist, B. H. Meier, and F. Merkt, Phys. Rev. A **75**, 31402 (2007).
[26] E. Narevicius, A. Libson, C. G. Parthey, I. Chavez, J. Narevicius, U. Even, and M. G. Raizen, Physical Review Letters **100**, 093003 (2008).
[27] E. Lavert-Ofir, S. Gersten, A. B. Henson, I. Shani, L. David, J. Narevicius, and E. Narevicius, New Journal of Physics **13**, 103030 (2011).
[28] K. Dulitz, M. Motsch, N. Vanhaecke, and T. P. Softley, The Journal of Chemical Physics **140**, 104201 (2014).
[29] Q. Wang, S. Hou, L. Xu, and J. Yin, Physical Chemistry Chemical Physics **18**, 5432 (2016).
[30] T. Cremers, S. Chefdeville, N. Janssen, E. Sweers, S. Koot, P. Claus, and S. Y. T. van de Meerakker, Phys. Rev. A **95**, 43415 (2017).
[31] V. Plomp, Z. Gao, T. Cremers, and S. Y. T. van de Meerakker, Physical Review A **99**, 33417 (2019).
[32] J. R. Bochinski, E. R. Hudson, H. J. Lewandowski, and J. Ye, Physical Review A **70**, 043410 (2004).
[33] B. C. Sawyer, B. L. Lev, E. R. Hudson, B. K. Stuhl, M. Lara, J. L. Bohn, and J. Ye, Physical Review Letters **98**, 253002 (2007).
[34] H. L. Bethlem, G. Berden, A. J. A. van Roij, F. M. H. Crompvoets, and G. Meijer, Physical Review Letters **84**, 5744 (2000).
[35] E. R. Hudson, J. R. Bochinski, H. J. Lewandowski, B. C. Sawyer, and J. Ye, The European Physical Journal D **31**, 351 (2004).
[36] See Supplementary Materials.
[37] E. L. Surkov, J. T. M. Walraven, and G. V. Shlyapnikov, Physical Review A **53**, 3403 (1996).
[38] S. Y. T. van de Meerakker, P. H. M. Smeets, N. Vanhaecke, R. T. Jongma, and G. Meijer, Physical Review Letters **94**, 023004 (2005).
[39] U. Even, Advances in Chemistry **2014**, 636042 (2014).
[40] H. Wu, D. Reens, T. Langen, Y. Shagam, D. Fontecha, and J. Ye, Physical Chemistry Chemical Physics **20**, 11615 (2018).
[41] H. Beijerinck and N. Verster, Physica B+C **111**, 327 (1981).